Available online at www.sciencedirect.com
SCIENCE DIRECT®
Journal of Theoretical Biology 238 (2006) 11–17
Journal of Theoretical Biology
www.elsevier.com/locate/yjtbi

Theoretical study on the body form and swimming pattern of *Anomalocaris* based on hydrodynamic simulation

Yoshiyuki Usami*

Institute of Physics, Kanagawa University, Rokkakubashi 3-27-1, Kanagawa 221-8686, Japan

Received 2 November 2004; received in revised form 29 April 2005; accepted 2 May 2005
Available online 6 July 2005

Abstract

Anomalocarid arthropod is the largest known predatory animal of middle Cambrian. Studies on *Anomalocaris* have been piled up in the past two decades since the first reasonable reconstruction had achieved in 1980s. Recent finding of legs beneath lobes on *Parapeytoia Yunnanensis* shows arthropod affinities, however, many researchers believe that it must be a powerful swimmer by the use of developed lobes. In this work, we investigate swimming behaviour of *Anomalocaris* in water by performing hydrodynamical calculation. As a result of simulation using moving particle method possible swimming motion of *Anomalocaris* is obtained. In the computer we can change the morphology from known bauplan of *Anomalocaris* found as fossil record. It makes us possible to discuss on the variants of *Anomalocaris* at the intermediate state of evolution process. Such new methodology using computer reveals how and from where *Anomalocaris* evolved.

Keywords: *Anomalocaris*; Theory; Hydrodynamics; Locomotion; Bauplan

1. Introduction

The story upon *Anomalocaris* is back to 1892 since Whiteaves described a part of this but not all of the body at first (Whiteaves, 1892). Walcott followed (Walcott, 1911), but understanding of its true nature should be waited until 1970s and 1980s when Conway-Morris, Briggs and Whittington re-examined it (Briggs, 1979; Briggs and Mount, 1982; Morris, 1982; Whittington and Briggs, 1985). At last, Whittington and Briggs achieved the first reasonable reconstruction of *Anomalocaris* in 1985. In 1980s and 1990s several researchers competitively revealed new features of anomalocarids including an introduction of new genera, and proposed new classifications (Bergstr, 1987; Chen et al., 1994; Hou and Bergstrom, 1995, 1997; Collins, 1996; Graham, 1998; Nedin, 1999). Those works presented a variation of the anomalocarids in many anatomical characteristics than previously assumed. For example some *Anomalocaris* such as *Parapeytoia Yunnanensis* had gnathobasic biramous trunk appendages, but no such appendages are found on the other major known *Anomalocaris*.

On the locomotion of *Anomalocaris*, traditional understanding of propulsion mechanism is sequential wavelike motion of the lobes. It is considered that the overlapped lateral lobes would work like the single lateral fin flap, so it might be resembling to a modern manta ray. Interpretation of the existence of biramous trunk appendages of a certain anomalocarid is problematic. It may be understood that primitive species still have endopod. However, on the course of evolution it lost endopod, but acquired developed exopod, i.e. lateral lobe. Majority of species having no endopod may imply that developed lateral lobes was an important organ so that *Anomalocaris* acquired propulsion.

Since *Anomalocaris* is considered as arthropod, discussion on locomotion should be made reflecting

*Tel.: +81 45 413 9771; fax +81 45 413 9771.
E-mail address: usami@kanagawa-u.ac.jp.

0022-5193/$ - see front matter © 2005 Elsevier Ltd. All rights reserved.
doi:10.1016/j.jtbi.2005.05.008

characteristics of arthropod body structure. However, there are few studies on arthropod swimming (Suter et al., 1997; Martinez et al., 1998), whereas studies on vertebrate locomotion in water have been piled up. Many experimental and theoretical studies have been achieved on aquatic vertebrate locomotion including fish (Lighthill, 1970; Wu, 1971; Vogel, 1994; Wolfgang et al., 1999), mammal (Fish, 1991), bird (Reilly et al., 1995; Hui, 1998), lizard (Farley and Christineko, 1997), etc. Recently, advanced computational ability has realized three-dimensional numerical simulation based on hydrodynamical theory. Wolfgang et al. successfully accomplished three-dimensional calculation of fluid dynamics around fish, and found good agreement with experimental data on water velocity (Wolfgang et al., 1999). However, when boundary of animal becomes complicate such as *Anomalocaris*, solving Navier-Stokes equation with moving boundary becomes hard task. Then, we employ moving particle method to solve hydrodynamical problem, which is proved to be equal to solve Navier-Stokes equation (Koshizuka et al., 1995, 1998; Koshizuka and Oka, 2001). Moving particle semi-implicit method is tracing virtual moving particle instead of solving nonlinear equation of velocity field. Physical quantities such as density of water, velocity and pressure are obtained from the information of moving particles. Calculation of the pressure is introduced to determine the motion of moving particle, which leads to good agreement between the calculation and experimental data of water motion (Chikazawa et al., 2001; Ikeda et al., 2001; Koshizuka et al., 1998; Yoon et al., 2001).

2. Computational method

Methodology of moving particle semi-implicit method is described in appendix with parameters. Numerical simulations are achieved in two-dimensional coordinate space. We consider a container as shown in Fig. 1 and put a model *Anomalocaris* in it. Lobe of *Anomalocaris* is modelled as plate which is expressed as line in two-dimensional simulation shown in the middle of Fig. 1. In this study the lobe changes its angle θ and vertical position H. By the introduction of phase difference ϕ_0 between lobes, ith lobe is assumed to change its angles θ_i and vertical position H_i as periodic function by

$$H_i(t) = H_0 \sin(\varpi t - i\phi_0),$$
$$\theta_i(t) = \theta_0 \cos(\varpi t - i\phi_0), \quad (1)$$

where H_0, θ_0 and ϖ are the amplitude of vertical motion, the angle and frequency, respectively. In the simulation, number of lobes is assumed as 11, because three frontal lobes are small in general and strongly overlapping behind the head among 14 lobes of *Anomalocaris*. As the given vertical motion with rotating angle series of lobe receives force from moving particle, which yields horizontal motion of model *Anomalocaris*. In the numerical analysis we measure two quantities which characterize *Anomalocaris* locomotion, i.e. swimming speed v, and energy loss E. We varied the parameters θ_0, ϕ_0 in the range of $20^\circ < \theta_0 < 60^\circ$ (with 10° step) and $20^\circ < \phi_0 < 40^\circ$ (with 5° step), and searched the optimized locomotion pattern. At first we give small width lobe for model *Anomalocaris*, and then see how they behave when we increase lobe width. The other parameters used in the simulation are summarized in Appendix A. Contribution from the other mode of sine function expressed in (Eq. (1)) is discussed in Appendix B.

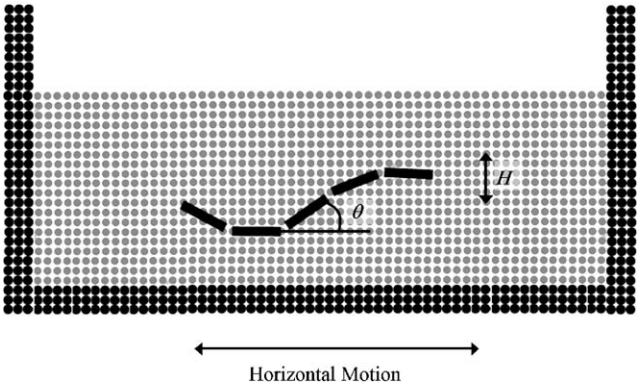

Fig. 1. Simulation setup for moving particle semi-implicit method. Simulation is performed in two-dimensional space. Moving particle expressed as grey is filled inside the container shown by black wall. Lobe of *Anomalocaris* is modelled by distinct plate which is expressed as bold line in two-dimensional space as shown at the middle of the container.

3. Swimming pattern of *Anomalocaris*

In Fig. 2 swimming speed and energy loss are plotted as the increase of lobe width. Energy loss E is assumed to be equal to surrounding water energy. Numerical simulation is performed in two-dimensional space, then another positional quantity is needed, i.e. depth of lobe to obtain the quantity of energy per second. Thus, energy unit is expressed as J/(s cm) in this work. Data points denoted as bracketed 3, 4, etc. in Fig. 2 expresses data for the case of lobe width as 3, 4 cm, etc. Corresponding three-dimensional structure of model *Anomalocaris* is schematically shown above data points. Among many sampling points of different ϕ_0 and θ_0, several data with larger values of v/E are plotted. The largest v/E motion expresses high-speed swimming in a energy saving manner. In Fig. 2 we observe the increase of both swimming speed and energy loss as the increase of lobe width. However, we notice great advance of swimming ability when lobe width reaches to 7 cm.

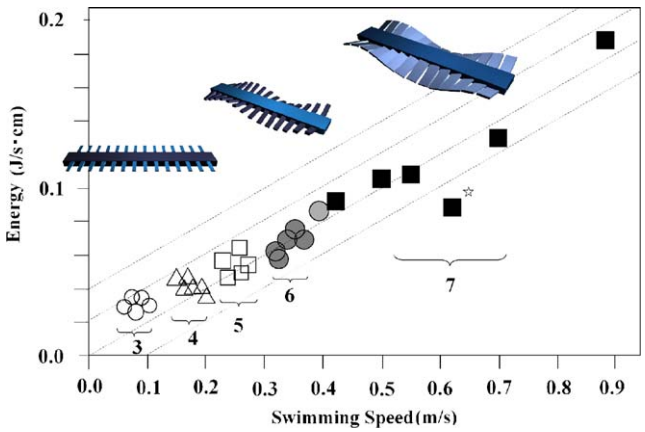

Fig. 2. Swimming speed and energy loss of *Anomalocaris*. Group of data point with bracketed number 3 expresses the one of *Anomalocaris* with 3 cm lobe width, for example. Corresponding 3D structure of model *Anomalocaris* is drawn on the data points. When lobe width grows from 3 cm to 4 cm, 5 cm, etc. swimming speed increases. Dashed line expresses proportional line of constant v/E. The data with the largest v/E is denoted with asterisk.

Maximum speed is 0.4 m/s for 6 cm width, however, swimming speed reaches to 0.9 m/s for 7 cm width. In this stage lobe of model *Anomalocaris* becomes like a continuous flap. Dashed line in Fig. 2 expresses proportional line of constant v/E. Black square with asterisk is the data which shows the maximum v/E among all data. In this case, model *Anomalocaris* can swim as the most efficient manner, which is realized when the structure of lobes becomes continuous. From fossil record we have observed overlapping structure of lobe in anomalocarid. Our calculation tells that such structure is logical consequence as pursuing locomotion ability among the variants of different bauplan of anomalocarids. Detailed discussion on the convergence of numerical simulation is summarized in Appendix C.

Several typical swimming patterns are plotted in Fig. 3. Velocity of moving particle is displayed as colored thick line. As for colour, low-velocity particle is shown as blue line, whereas fast moving particle is shown as red. Figs. 3A–C show snapshots of the swimming pattern whose data point is shown with asterisk in Fig. 2. Corrective motions of water denoted as G1 and G2 generate propulsion force of model *Anomalocaris* for going forward (right-hand side). Repulsive motion of water from lobes denoted as G3 is observed as a result of waving pattern. It is interesting to observe that snapshot of waving lobe resembles to be a continuous single flap. The 11 lobes are given as

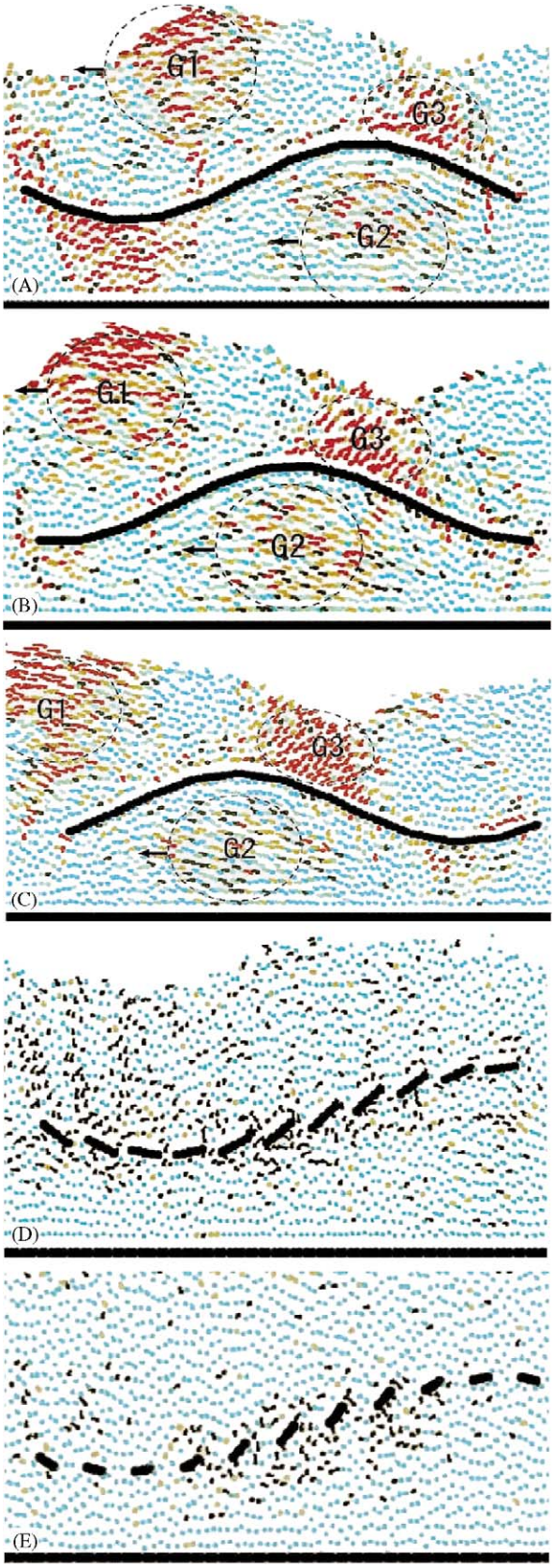

Fig. 3. The optimal locomotion of model *Anomalocaris*. Motion of A–C corresponds to the one of the data with asterisk in Fig. 3. Overall behaviour of distinct flap becomes like single continues flap. Groups of water environment labelled as G1 and G2 move to left side, then model *Anomalocaris* acquires propulsion for going to right side. (D and E) Swimming pattern of ancestral *Anomalocaris* which is assumed to have distinct under developed lobe. Excessive waving motion for each lobe is observed.

distinct ones in the simulation, however, successive lobes behave as a single flap in the optimized locomotion. On the contrary, no such continuous wave pattern is observed for the other structure of the lobe (Figs. 3D–E). We even notice that excess waving motion of each lobe is observed, which is efficient as swimming locomotion for under evolved *Anomalocaris*. By far many paleontologists have stated that lobe of *Anomalocaris* are overlapped, and it would work like the single lateral fin flap. Then we can conjecture from our hydrodynamic simulation that the structure of *Anomalocaris*' overlapped lobes is originated by pursuing the optimal swimming locomotion with maximizing v/E, i.e. high-speed motion with small energy.

4. Evolution of *Anomalocaris*

On the evolution of lobe of *Anomalocaris* possible morphological change could be classified into the following three patterns as summarized in Fig. 4. Type 1: At first tiny thin appendage is generated perpendicular to the body, and then its width increases through evolution (Figs. 4A–C). Type 2: Primitive *Anomalocaris* already had broad lobe (Fig. 4D), and then depth of lobe gradually grows as Figs. 4(D)–(C). Type 3: Primitive *Anomalocaris* had fewer lobes than the completed form of 14 lobes (Fig. 4F). However, number of lobes increases through evolution up to the final form of *Anomalocaris*, whose evolutional pattern is similar like trilobite development (Forty, 2001).

To judge fairly characteristics of these three, type 3 requires systematic genetic change compared to the change of size of a organ in Types 1 and 2. So it might be said that evolution by the pass of Type 1 or Type 2 is plausible than the structural change of Type 3. In many

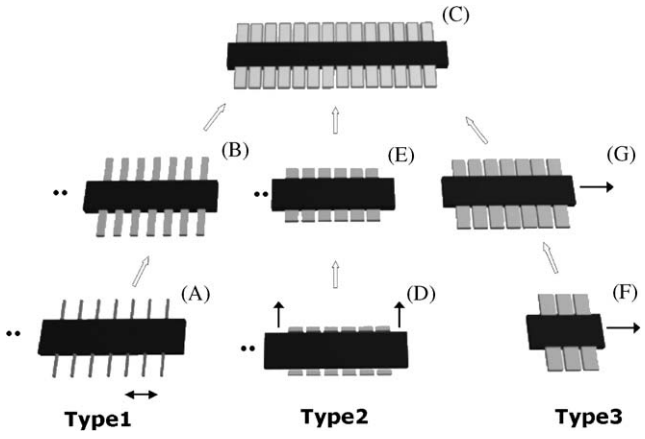

Fig. 4. Possible schemes on the evolution of lobes of *Anomalocaris*. Type 1; appendage evolved perpendicular to the body, at first and then the width of it increases. Type 2; broad lobe is created, at first and then the length of it grows. Type 3; small number of segmented structure is created, at first. Then number of segments is increased.

arthropod-like fauna of the middle Cambrian we have found many creatures whose basic bauplan has the form of Fig. 4A. Such baulplan is suitable for walking on the sea bottom. On the contrary, function of lobe of Fig. 4D is not clear. The bauplan of Fig. 4D would be inconvenient for both walking and swimming if primitive *Anomalocaris* had such lobes. Then, we can conclude that the morphological change of the appendage to evolved lobe on the pass of Type 1 is the most plausible path for *Anomalocaris*. Quantitative advantage through morphological change of Type 1 is by far presented in our numerical calculations.

5. Conclusion

In the present work we have shown that we could simulate and discuss how extinct animal behaved and evolved, which is not reserved as fossilized remains, using computer. As a result we have revealed that *Anomcalocaris*' developed overlapping lobe is a logical consequence of pursuing swimming ability. And we have shown that *Anomalocaris* would wave their lobes as continuous single flap, which is the optimal swimming motion.

At present time, we observe functionary the same body plan of *Anomalocaris* in manta ray whose origin is totally different from the present case, but we recognize adaptive evolutionary convergence of the body plan between them. It is amazing that creature lived in the period of Cambrian explosion 530 million years ago already reached to have matured sophisticated body form.

Acknowledgements

This research was partially supported by the Ministry of Education, Science, Sports and Culture, Grant-in-Aid for Scientific Research (C)-15570022.

Appendix A

In this appendix section we describe briefly moving particle semi-implicit method and parameters used in this work. Discussion on the validity of each quantity in the simulation is also discussed.

Let $D\vec{u}/Dt$ be the Lagrange time derivative to the velocity field of water $\vec{u}$. Then fluid dynamics is described by solving Navier-Stokes equation

$$\frac{D\vec{u}}{Dt} = -\frac{1}{\rho}\nabla P + \nu\nabla^2\vec{u} + \vec{F}, \tag{A.1}$$

where P, $\vec{F}$, ρ and ν are pressure, external force, density and kinetic viscousity constant, respectively.

Alternatively, Koshizuka and Oka proposed dynamics of moving particle method (Koshizuka et al., 1995, 1998; Koshizuka and Oka, 2001). In the moving particle method a particle has a weight function to restrict the particle interaction with a finite radius of r_e

$$w(r) = \begin{cases} r_e - 1 & r < r_e, \\ 0 & r_e < r, \end{cases} \tag{A.2}$$

where r is the distance between two particles. Fluid density is represented by particle number density n at the particle i with the use of weight function of particle i and its neighbor j as, $n_i = \sum_{j \neq i} w(\vec{r}_j - \vec{r}_i)$. Diffusion is modelled by distribution of part of a quantity from a particle i to its neighbor particle j by the use of the weight function as

$$\nabla^2 \vec{u}_i \propto \frac{1}{n^0} \sum_{j \neq i} (\vec{u}_j - \vec{u}_i) w(\vec{r}_j - \vec{r}_i). \tag{A.3}$$

When we have n step velocity $\vec{u}_i^n$ and position $\vec{r}_i^n$, next we calculate temporal ones $\vec{u}_i^*$ and $\vec{r}_i^*$, as

$$\vec{u}_i^* = \vec{u}_i^n + \Delta t (\nu \nabla^2 \vec{u}_i^n + \vec{F}), \tag{A.4}$$

$$\vec{r}_i^* = \vec{r}_i^n + \vec{u}_i^* \Delta t. \tag{A.5}$$

By an introduction of correction of velocity $\vec{u}_i'$, next time step velocity and position are obtained as

$$\vec{u}_i^{n+1} = \vec{u}_i^* + \vec{u}_i', \tag{A.6}$$

$$\vec{r}_i^{n+1} = \vec{r}_i^* + \vec{u}_i' \Delta t. \tag{A.7}$$

As a result of the calculation of (A.4) and (A.5), number density becomes temporal one as n^*. Then we need to correct number density to the correct one of the system n^0 as, $n^0 = n_i^* + n_i'$, where $n'$is a correction such that the system keeps number density n^0. Velocity correction $\vec{u}_i'$ should be calculated by the pressure gradient as

$$\vec{u}_i' = -\frac{\Delta t}{\rho} \nabla P^{n+1}. \tag{A.8}$$

Momentum conservation low requires for $\vec{u}_i'$ and n' as the following:

$$\frac{n_i'}{\Delta t} + \nabla \cdot (n^0 \vec{u}_i') = 0. \tag{A.9}$$

Then we have an expression of Poisson equation from (A.8) and (A.9) in the particle method as

$$\nabla^2 P_i^{n+1} = -\frac{\rho}{\Delta t^2} \cdot \frac{n_i^* - n^0}{n^0}. \tag{A.10}$$

Eqs. (A.4)–(A.7) and Eq. (A.10) is a equivalent expression in moving particle method as Navier-Stokes equation.

Let us summarize the parameter used in this work. At first, note that Navier-Stokes equation yields to the dimensionless form as the following by the introduction of characteristic length L_0, velocity V_0, pressure P_0 and force F_0:

$$\frac{\tilde{\mathrm{D}}\vec{\tilde{u}}}{\tilde{\mathrm{D}}\tilde{t}} = -\tilde{\nabla}\tilde{P} + \frac{1}{Re} \tilde{\nabla}^2 \vec{\tilde{u}} + \vec{\tilde{F}}, \tag{A.11}$$

where variable with tilde expresses dimensionless as $\tilde{\nabla} = \nabla L_0, \vec{\tilde{u}} = \vec{u}/V_0, \vec{\tilde{F}} = \vec{F}/F_0, \quad \tilde{P} = P/P_0$. $Re = V_0 L_0/\mu$ is a dimensionless parameter called Reynolds number. Let us assume that characteristic length of the system is $L_0 = 0.6\,\mathrm{m}$ which is the size of known largest *Anomalocaris*. If we assume swimming speed of the creature as $V_0 = 1\,\mathrm{m/s}$, and $\mu = 1.0 \times 10^{-6}\,\mathrm{m^2/s}$, then we have $Re = 5 \times 10^5$. We use this value as Reynolds number. Characteristic radius of moving particle used in the simulation is 0.5 cm. In a simulation width of lobe is varied from 2 to 7 cm. Number of lobes is given as 11, which leads to maximum size of the body as 77 cm. Width of container is 1.7 m presented in this work, however, we have accomplished several test calculations by changing this size. The results show essentially similar to the ones presented in this paper. Vertical motion of lobe is given as the expression (Eq. (1)) with the amplitude $H_0 = 3.5\,\mathrm{cm}$ which is half size of the lobe width. Water particle receives gravitational force vertically downward direction as $F_0 = 9.8\,\mathrm{m/s}$. Then lobe receives reaction force from water particle, then it moves horizontal direction. Swimming speed obtained in the calculation becomes 0.1–1 m/s which is shown in Fig. 2. When we refer to fish locomotion, power law for swimming speed and body length is known. For example, it shows 0.3 m/s speed for 0.1 m fish, and 1 m/s speed for 1 m fish as lower case. Our results show almost similar value of these vertebrate references. But it is known that velocity of fast swimming fish reaches to 10 m/s. The simulation is performed in two-dimensional space, then energy expression used in the text has the unit [J/(cm s)]. We must assume depth of lobe to obtain the ordinary energy unit [J/s]. If we assume the lobe width as 10 cm, swimming energy becomes 0.2–2 J/s from Fig. 2. Again as for vertebrate reference, it is known that 0.3 m body length carp swims 0.98 m/s speed with 0.4 J/s energy. Our calculation shows similar order in energy spent with vertebrate example.

Appendix B

In this section we comment on contribution from the other mode of sine function expressed as Eq. (1). In our previous work (Usami, 1998) we also studied swimming motion of *Anomalocaris*, however, the method used in the work is different from the present study. First, our previous work (Usami, 1998) did not calculate solvent motion. Instead, only force from fixed frame is considered. Then, fluid energy could not be obtained because of absence of knowledge of fluid motion. Second, motion of lobe is assumed to rotate around

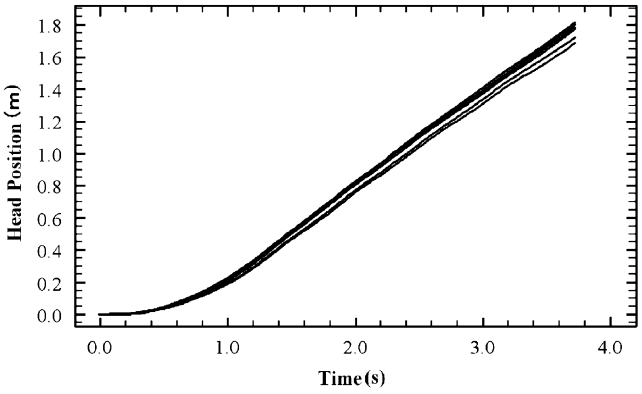

Fig. B.1. Head position of model *Anomalocaris* versus time. Seven samples are plotted in this figure. Overlapped profiles show steady and similar swimming motion of each example. Parameters appeared in this work are the same, however, surrounding solvent relaxation is different.

joint according to following expression:

$$\theta x(t) = a_1^1 \cos(\varpi_1^1 t + \delta_1^1) + a_2^1 \cos\left(\varpi_2^1 \frac{1}{2} t + \delta_2^1\right),$$

$$\theta y(t) = a_1^2 \cos(\varpi_1^2 t + \delta_1^2) + a_2^2 \cos\left(\varpi_2^2 \frac{1}{2} t + \delta_2^2\right),$$

$$\theta z(t) = a_1^3 \cos(\varpi_1^3 t + \delta_1^3) + a_2^3 \cos\left(\varpi_2^3 \frac{1}{2} t + \delta_2^3\right), \quad \text{(B.1)}$$

where θx, θy, θz and t represents angle around x, y, z axes and time, respectively. In the work optimized motion is obtained by the use of evolution algorithm for the parameters set $a_1^1, a_2^1, \varpi_1^1, \varpi_2^1, \delta_1^1, \delta_2^1, \ldots$. Then, the author found that contribution from the first term is much larger than the second term, i.e. the values of a_1^1, a_1^2, a_1^3 are much larger than a_2^1, a_2^2, a_2^3. Consequently, waving pattern of lobe is looked like the sine function. Many strange motions appear in the calculation of evolution algorithm, which have similar value of a_1^1, a_1^2, a_1^3 and a_2^1, a_2^2, a_2^3, those are not the optimal solution as a function of swimming speed. In the present framework surrounding fluid environment has a mechanism to prevent rapid motion of the object. Furthermore, smooth wavy pattern of series of 11 lobes brings stable swimming motion which is clearly observed in Fig. B.1. Then, considering only the first term of Eq. (B.1) is adequate for discussing motion of series of lobe in surrounding fluid environment.

Appendix C

In this section we describe on the convergence of numerical simulation. For the data of most efficient swimming style denoted as asterisk in Fig. 2 we calculate 7 examples of swimming motion. All the parameter appeared in this work is fixed, however, initial relaxation

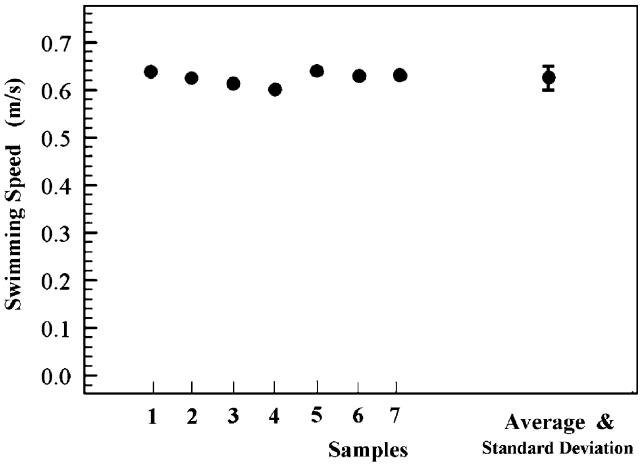

Fig. C.1. Swimming speed of seven examples is plotted at the left. Average speed with standard deviation is also shown at the right. The value of speed is $v = 0.62 \pm 0.01$ m/s. This graph shows small fluctuation among samples and small standard deviation.

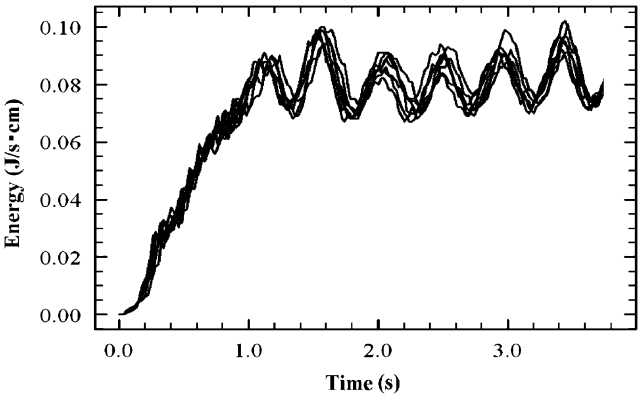

Fig. C.2. Energy profile of seven different swimming motion. Initial stage from 0 to 1.2 s shows transition from the rest position to steady state swimming motion. The later process shows steady state of swimming motion of model *Anomalocaris*. Oscillatory pattern of energy profile is caused by waving motion of the lobe of model *Anomalocaris*.

of solvent motion is different. For checking convergence of swimming speed, we plot head position of *Anomalocaris* in Fig. B.1. From this figure, we clearly observe stable and similar behavior of swimming motion. Smooth wavy pattern of 11 lobes is considered to bring stable motion of object. Swimming speed for each example is plotted in Fig. C.1. Average speed of seven examples with standard deviation is also shown in Fig. C.1. We can observe that fluctuation of speed of each example is small, which yields small value of standard deviation as $v = 0.62 \pm 0.01$ m/s.

Fig. C.2 displays energy profile of these seven examples of swimming motion. In this figure we observe similar behaviour of energy profile. The pattern of time duration from 0 to 1 s shows initial stage of the motion from the rest position to steady state. For time duration

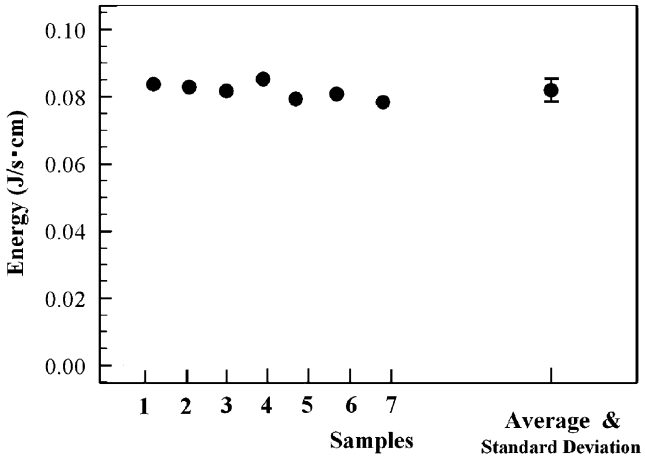

Fig. C.3. Averaged energy for each sample is plotted at the left. Average energy over seven samples is shown with standard deviation at the right. The energy is calculated as $0.082 \pm 0.002\,\mathrm{J/(s\,cm)}$. Small standard deviation is also observed from this figure.

from 1.2 to 4.0 s steady state of energy profile is observed, which corresponds to steady state of swimming motion. Wavy pattern of lobe of *Anomalocaris* makes oscillatory pattern of energy profile for the later stage of simulation. Fig. C.3 summarizes average energy during steady state of these seven examples. The value of average over seven examples is $0.082 \pm 0.002\,\mathrm{J/(s\,cm)}$. Fluctuation of examples is relatively small, it supports validity of our simulation results through this work.

These calculations are accomplished on 6000 particles simulation. The computation time needed for each example reaches almost 6 h using the fastest personal computer available in the year of 2004 (3.0 GHz dual Xeon processor. with Redhat 9.0 operating system).

References

Bergstr, J., 1987. The Cambrian Opabinia and Anomalocaris. Lethaia 20, 187–188.

Briggs, D.E.G., 1979. *Anomalocaris*, the largest known Cambrian Arthropod. Paleontology 20, 631–664.

Briggs, D.E.G., Mount, D.J.D., 1982. The occurrence of the giant arthropod *Anomalocaris* in the Lower Cambrian of Southern California, and the overall distribution of the genus. J. Paleontol. 56, 1112–1118.

Chen, J.-y., Ramskold, L., Zhou Guiquing, 1994. Evidence for monophyly and arthropod affinity of Cambrian giant predators. Science 264, 1304–1308.

Chikazawa, Y., Koshizuka, S., Oka, Y., 2001. Numerical analysis of three dimensional sloshing in an elastic cylindrical tank using moving particle semi-implicit method. Comput. Fluid Dyn. J. 9, 376–383.

Collins, D., 1996. The 'Evolution' of *Anomalocaris* and its classification in the arthropod Class Dinocardia (NOV.) and Order Radiodonta (NOV.). J. Paleontol. 70, 280–293.

Farley, C.T., Christineko, T., 1997. Mechanics of locomotion in lizards. J. Exp. Biol. 200, 2177–2188.

Fish, F.E.H., 1991. Dolphin swimming—a review. Mammal Rev. 21, 181–195.

Forty, R., 2001. Eyewitness to Evolution. Vintage Books.

Graham, E.B., 1998. Arthropod body-plan evolution in the Cambrian with an example from Anomalocaridid nuscle. Lethaia 31, 197–210.

Hou, X., Bergstrom, J., 1995. *Anomalocaris* and other large animals in the Lower Cambrian Chengjiang fauna of southwest China. GFF 117, 163–183.

Hou, X., Bergstrom, J., 1997. Arthropods of the Lower Cambrian Chengjiang fauna, southwest China. Fossils Strata 45, 1–116.

Hui, C.A., 1998. Penguin swimming, I. Hydorodynamics. Physiol. Zool. 61, 333–343.

Ikeda, H., Koshizuka, S., Oka, Y., Park, H.S., Sugimoto, J., 2001. Numerical analysis of jet injection behavior for fuel-coolant interaction using particle method. J. Nucl. Sci. Tech. 38, 174–182.

Koshizuka, S., Oka, Y., 2001. Application of moving particle semi-implicit method to nuclear reactor safety. Computat. Fluid Dyn. J. 9, 366–375.

Koshizuka, S., Tamako, H., Oka, Y., 1995. A particle method for incompressible viscous flow with fluid fragmentation. Computat. Fluid Dyn. J. 4, 29–46.

Koshizuka, S., Nobe, A., Oka, Y., 1998. Numerical analysis of breaking waves using the moving particle semi-implicit method. Int. J. Numer. Methods Fluids 26, 751–769.

Lighthill, M.J., 1970. Aquatic animal propulsion of high hydromechanical efficiency. J. Fluid Mech. 44, 265–301.

Martinez, M.M., Full., R.J., Koehl, M.A.R., 1998. Underwater punting by an intertidal crab: A novel gait revealed by the kinematics of pedestrian locomotion in air versus water. J. Exp. Biol. 201, 2609–2623.

Morris, S.C., 1982. The enigmatic medusoid Peytoia and a comparison of some Cambrian biotas. J. Paleontol. 56, 116–122.

Nedin, C., 1999. "*Anomalocaris*" predation on mineralized and non-mineralized trilobites. Geology 27, 987–990.

Reilly, P., Dann, P., Norman, I. (Eds.), 1995. The Penguins. Hyperion Books.

Suter, R.B., Rosenberg, O., Loeb, S., Wildman, H., Long, J.H., 1997. Locomotion on the water surface: propulsive mechanisms of the fisher spider Dolomedes Triton. J. Exp. Biol. 200, 2523–2538.

Usami, Y., 1998. Reconstraction of Extinct Animals in the Computer. Artificial Life VI. The MIT Press, Cambridge, MA, pp. 173–177.

Vogel, S., 1994. Life in Moving Fluids. Princeton University Press, Princeton, NJ.

Walcott, C., 1911. Middle cambrian annelids. Cambrian geology and paleontology. II. Smithson. Misc. Coll. 57, 109–134.

Whiteaves, J.F., 1892. Description of a new genus and species of Phyllocarid Crustacea from the Middle Cambrian of Mount Stephen, B.C. Can. Record Sci. 5, 205–208.

Whittington, H.B., Briggs, D.E.G., 1985. The largest Cambrian animal, *Anomalocaris*, Burgess Shale, British Columbia. Phil. Trans. Roy. Soc. London Series B. 309, 569–609.

Wolfgang, M.J., Anderson, J.M., Grosenbaugh, M.A., Yue, D.K.P., Triantafyllou, M.S., 1999. Near-body flow dynamics in swimming fish. J. Exp. Biol. 202, 2303–2327.

Wu, T.Y., 1971. Hydromechanics of swimming propulsion. Part 1 Swimming of a two dimensional flexible plate at variable forward speeds in an inviscid fluid. J. Fluid Mech. 46, 337–355.

Yoon, H.Y., Koshizuka, S., Oka, Y., 2001. Direct calculation of bubble growth, departure and rise in nucleate boiling. Int. J. Multiphase Flow 27, 277–298.